

ANALYSIS OF POOL BOILING IN MICROGRAVITY DURING LOSS OF COOLING FOR THE QUENCH MODULE INSERT (QMI)



Richard D. Horton
Tec-Masters, Inc.

ABSTRACT

In support of the thermal design of the quench module insert (QMI) microgravity experiment, a thermal/fluid math model was created with SINDA/FLUINT in order to simulate a loss of cooling scenario and the resultant pool boiling in the cooling lines. The objectives of the analysis were to determine whether critical components would surpass maximum temperature, what affect would phase change have on the component temperatures, and how much liquid volume would be expelled during the phase change. While developing the model, concerns were raised about the validity of phase change correlations used in SINDA/FLUINT when applied in the microgravity environment. This paper discusses the results of the thermal/fluid math model and the impact of microgravity on the pool boiling heat transfer coefficient.

INTRODUCTION

The QMI is a high gradient vacuum furnace, which will be used to perform directional solidification experiments in a microgravity environment. It will be installed in the Microgravity Science Laboratory (MSL) housed within the Materials Science Research Rack-1 (MSRR-1) aboard the International Space Station (ISS). This will be one of the first science facilities installed on the ISS¹. The QMI is made up of four heated zones and one water-cooled zone, which produces a high thermal gradient in a metal/alloy sample rod. The overall QMI design consists of a hot zone, a cold zone, a gradient zone, a quench zone, an insulation jacket, and coolant loops¹. The hot zone is made up of four independently controlled heaters insulated by alumina core sleeves within a Tantalum core housing (see figure 1). The hot zone assembly is designed to operate at a maximum temperature of 1400°C. The cold zone consists of a water-cooled copper outer-sleeve (chill block) coupled to an aluminum inner-sleeve through a conical interface. The inner-sleeve, known as the Thermal Interface Collar (TIC), interfaces with the Sample/Ampoule/Cartridge Assembly (SACA) through a high conductance material known

as Veltherm™. A variable flow rate water loop provides cooling to the chill block. The gradient zone consists of twenty molybdenum radiation shields, which provide axial isolation between the hot and cold zones. The quench zone is attached to the TIC of the cold zone and consists of a phase change device and actuation mechanism as shown in figure 1. The quench zone provides for a rapid cooling of the SACA material; however, for the purposes of this analysis, a non-quench TIC was used. The insulation jacket consists of two ten-layered spirally wrapped jackets of molybdenum foil. The hot zone, gradient zone, and insulation jacket are all mounted within the furnace housing. The furnace housing is cooled by a constant flow rate water loop that is brazed onto the housing jacket in a helical pattern (figure 1).

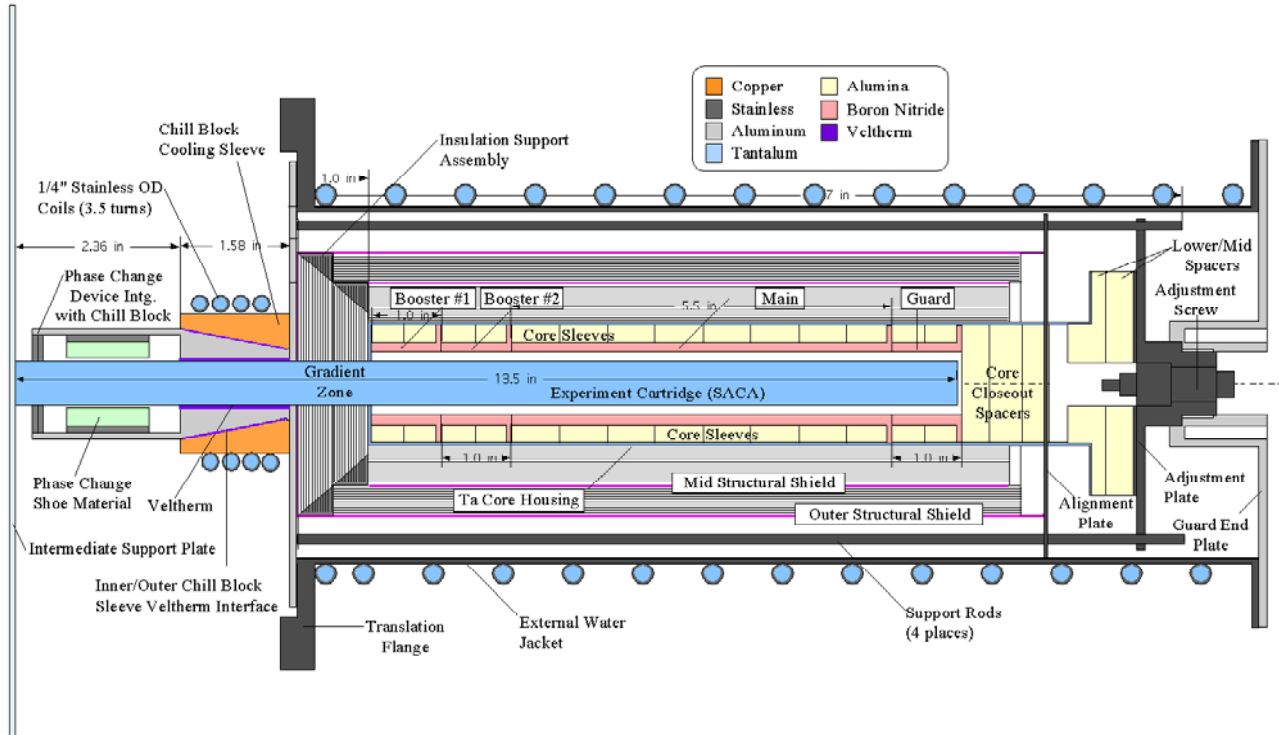


Figure 1: QMI cross-section¹

A requirement of the QMI design is that the furnace does not cause any damage to the vacuum chamber during a loss of cooling event. The loss of cooling scenario that was envisioned was one in which a failure of the cooling loop pump halts the coolant flow. The heaters remain operational until a set point is reached by one of several monitored thermocouples placed on or near critical components. Critical temperatures for these components are reached almost immediately after the water flow stops. Thus, a loss of cooling quickly results in a loss of power. Once the power has been shut off, the furnace is then allowed to cool through radiation and conduction to the experiment chamber walls.

To ensure that a loss of cooling event would not damage the experiment chamber, a thermal math model was developed to simulate the loss of cooling scenario. Furthermore, it was hoped that the math model results could be used to develop possible design solutions that would enable the furnace to survive the loss of cooling event and maintain subsequent operational capability. The math model results were used to obtain maximum heat fluxes from the furnace to the experiment chamber and maximum furnace component temperatures.

MODEL DESCRIPTION

The original thermal math model for the QMI was developed using SINDA/G and TRASYS. The fluid portion of the model consisted of one-way conductors whose values were updated through the use of Fortran subroutines. Two simple FLUINT models, one for each cooling loop, had also been developed separately from the SINDA/G thermal model. These two models used heat flux arrays generated from the thermal model to impose heat loads directly onto the fluid lumps. This method allowed for an estimate of water volume expulsion and an approximation of when boiling in the cooling lines would begin to occur after the pump failure. To simulate loss of cooling, the steady state temperatures from the SINDA/G thermal model were used as initial conditions and radial conduction replaced the film coefficient calculations from the tube wall nodes to the fluid nodes. The model was then run using a transient solution routine until maximum temperatures for the critical components were reached. At that point, the heaters shut off and the transient run terminated. The results from this solution were then used as initial conditions for a second transient solution in which the water nodes were completely removed. This model was then used to simulate the transient heat up and eventual cool down of the furnace after the water had completely boiled. This conservative method of simulating phase change ignores the energy storage experienced due to the latent heat of vaporization.

In an effort to produce less conservative results that would more realistically predict maximum temperatures, a fully integrated thermal/fluid model was developed using SINDA/FLUINT. Since the two cooling loops for the furnace share a common outlet, a single fluid network was created to allow fluid exchange from one loop to another. The thermal and fluid models were integrated through the use of heat transfer ties². Theoretically, this technique would provide a more accurate simulation of the phase change heat transfer as well as the volume expulsion that would take place in the cooling lines as the water flow stopped and the furnace begins to overheat. In addition to the heat transfer and thermal expansion of the fluid, this method would simulate the transient affects produced by the energy storage due to the heat of vaporization.

The thermal nodalization of the coolant tubing consists of three parts: an inner surface arithmetic node, a centerline diffusion node and an outer surface arithmetic node. The water jacket tubing is represented by four node groups for every 360° loop and one node group each for inlet and outlet routing. The chill block tubing is represented by a single node group for every 360° loop while the inlet and outlet routing is represented by an additional ten node groups, which includes the combined outlet tubing for the chill block and water jacket (figure 2). The diffusion nodes are connected by linear conductors to provide axial conduction within the tubing. The fluid model consists of fluid tank lumps, which correspond to each inner surface thermal node and are connected by inter-model heat transfer ties². The tanks are connected by tubes that provide a flow path for thermal expansion of the water during conductive heating and expulsion of the water during boiling. Plenums were used to represent the supply and outlet of the cooling system. The thermal model is much more complex and a full description is beyond the scope of this paper. Due to science requirements imposed by the experiments for which the QMI was designed, the thermal model consists of nearly 5000 nodes. One of the keys to the directional solidification experiment is knowing the exact location of the solid/liquid interface. The accuracy required to locate the solid/liquid interface resulted in an axial nodal resolution of 2 millimeters.

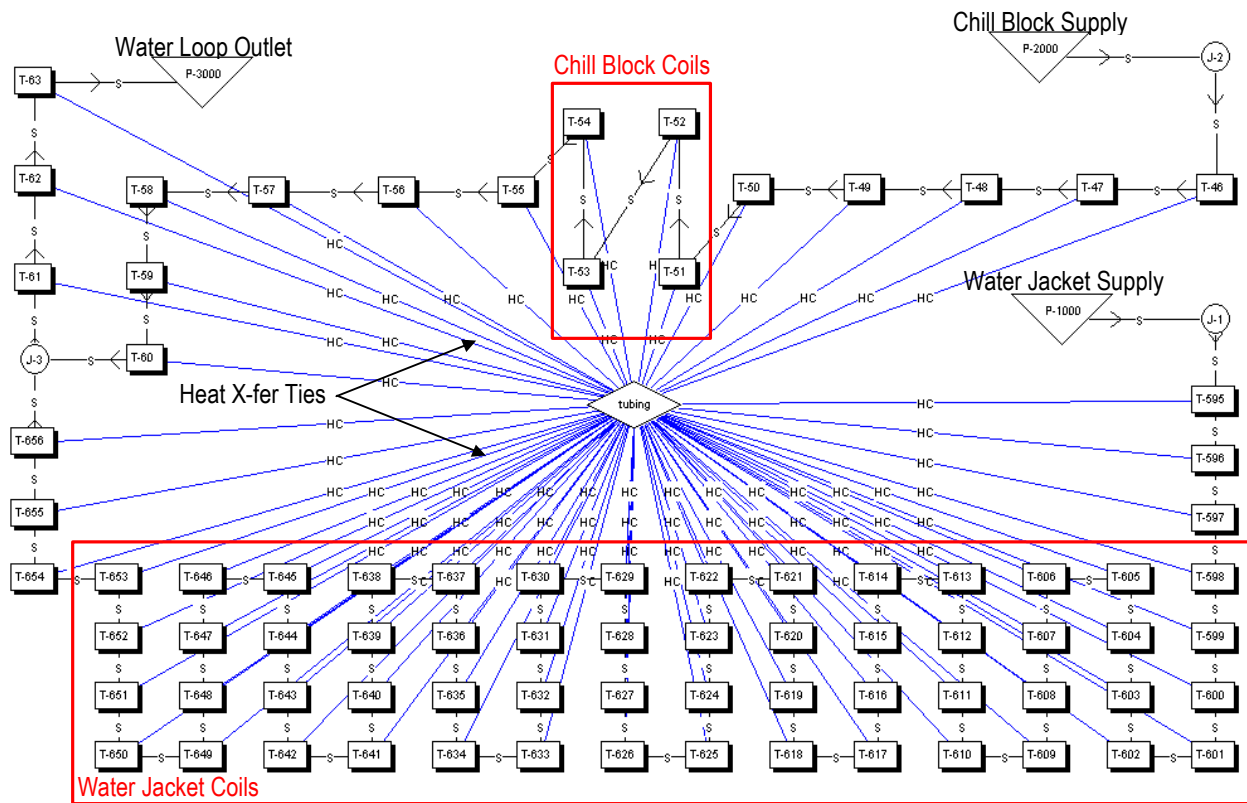


Figure 2: Fluid Model Network Diagram

POOL BOILING HEAT TRANSFER

As was mentioned in the preceding section, phase change provides a means of energy storage. During a loss of cooling scenario, the heat transfer rates from the furnace to the chamber become critical. By using the energy storage of the water in the cooling loops, it may be possible to reduce the maximum heat transfer rates and spread the heat transfer over a longer time period so as to avoid over heating the chamber as well as the furnace. However, it was unknown what differences may exist between boiling on Earth and boiling in low Earth orbit (LEO) or what affects any differences may have on the boiling heat transfer coefficients.

CORRELATIONS IN EARTH GRAVITY

The subject of pool boiling in a 1-g environment has been covered extensively in engineering research and testing. Numerous correlations have been developed for the purpose of describing the effects of phase change heat transfer analytically. Since these correlations were empirically derived from test data, they are very specific with respect to the geometry and conditions under which the tests were performed. Thus, any analysis performed with these

correlations on conditions other than those for which the correlations were derived will produce additional uncertainty in the results on top of that which is inherent to this type of analysis. Unfortunately, pool boiling inside tubes is not a situation that has received much if any attention by the research community. While correlations may exist for pool boiling in tubes, the only correlations that were found in preparation for this analysis pertained to forced convection or flow boiling. Therefore, the correlations for a flat plate will be used for this analysis.

Before beginning a discussion on the various correlations for all phases of boiling heat transfer, a discussion of the various boiling regimes is warranted. These regimes can best be described through an examination of the boiling curve (see figure 3)⁴. For the segment AB in the boiling curve, single-phase convection is the only form of heat transfer that occurs. As the heated surface temperature exceeds the saturation temperature of the liquid, bubbles begin to form in surface cavities and nucleate boiling begins. As the bubbles are removed from the surface by buoyancy forces, cooler liquid flows back into the cavity and the process continues. The sudden increase in heat transfer due to the removal of latent heat during vaporization results

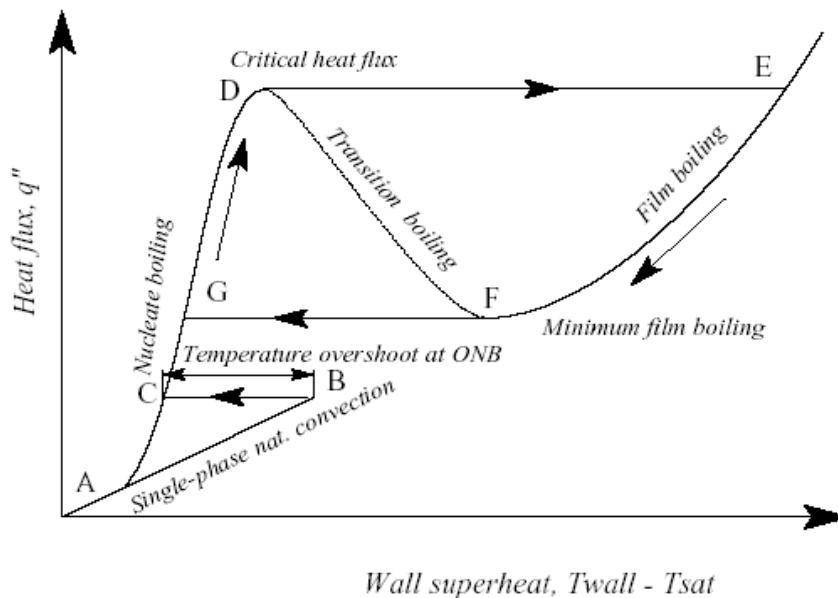


Figure 3: Typical Boiling Curve⁴

in a sudden drop in wall superheat at the onset of nucleate boiling (ONB) which is denoted by path BC in the curve. Path CD represents the nucleate boiling regime and during this period more and more bubbles are formed at the surface. As can be seen from the curve, in the nucleate boiling regime the wall superheat changes very slowly for a rapid increase in surface heat flux. As the wall superheat reaches the critical heat flux (CHF), a transition to film boiling begins represented by path DF. If the wall superheat is increased rapidly up to the critical heat flux, a direct jump to full film boiling may occur (path DE). The transition boiling regime is very unstable, and at any point on the surface the process can oscillate between nucleate and film boiling. This phenomenon is known as a hysteresis loop and can cause significant problems when attempting to model this transition boiling⁵. As can be gathered from the previous description, the phenomena that occur during boiling heat transfer are very complex and some aspects are still not very well understood. Analytical and empirical investigations into these phenomena are the subject of ongoing research.

The analytical process for the nucleate boiling phase begins with Newton's law of cooling³,

$$q_s'' = h(T_{\text{wall}} - T_{\text{sat}})$$

where q_s'' is the surface heat flux and $\Delta T_e = (T_{\text{wall}} - T_{\text{sat}})$ is the excess temperature. If these two values are known then the heat transfer coefficient, h , can be calculated from the above equation. Using the flat plate as the geometry baseline, the surface heat flux can be calculated from the well-known correlation that was developed by Rohsenow³.

$$q_s'' = \mu_l h_{\text{fg}} \left[\frac{g(\rho_l - \rho_v)}{\sigma} \right]^{1/2} \left(\frac{c_{p,l} \Delta T_e}{C_{s,f} h_{\text{fg}} \text{Pr}_l^n} \right)^3$$

The coefficient $C_{s,f}$ and the exponent n are dependent upon the surface-liquid combination. For stainless steel tubes filled with water, representative values are 0.06 and 1.0 respectively³. An important point on the boiling curve is the critical heat flux (CHF) at which point nucleation begins to be replaced by a constant vapor film between the surface and the liquid. Knowing when this phenomenon will begin to occur is of vital importance in preventing "burnout" which can damage the heating surface, as the vapor will act as an insulator. This is not a concern in the loss of cooling situation for QMI. However, the critical heat flux is important in that it is a signal that the correlation for nucleate boiling can no longer be used to calculate heat transfer. Through a hydrodynamic stability analysis, Zuber obtained an expression for determining the critical heat flux, which was independent of surface material and only weakly dependent on geometry³. Through experimentation and approximation the correlation was later refined to:

$$q_{\text{max}}'' = 0.149 \cdot h_{\text{fg}} \rho_v \left[\frac{\sigma g (\rho_l - \rho_v)}{\rho_v^2} \right]^{1/4}$$

The transition boiling regime is generally only obtainable by controlling the heated surface temperature, and no reliable correlation for predicting heat transfer exists at this time⁶. It is more widely assumed that at the CHF, film boiling begins. This phase of boiling is a combination of heat transfer through a vapor layer and radiation to fluid from heated surface. During film boiling, the temperature of the heated surface begins to increase rapidly since the heat transfer path is now primarily through the insulating vapor layer. The correlation for film boiling that was available in the text is for the geometry of horizontal cylinders immersed in a fluid and was developed by Bromley⁵.

$$\text{Nu}_D = \frac{h_b D}{k_v} = 0.62 \left[\frac{g \rho_v (\rho_l - \rho_v) (h_{\text{fg}} + 0.4 c_{p,v} \Delta T_e) D^3}{\mu_v k_v \Delta T_e} \right]^{1/4}$$

Vapor properties in the above equation are evaluated at the film temperature and the liquid density is evaluated at the saturation temperature. The variable, h_b , is the boiling heat transfer

coefficient as opposed to the radiation heat transfer coefficient, h_r , which becomes a more significant contributor to the overall heat transfer at surface temperatures above about 300°C. The radiation heat transfer coefficient can be calculated from the equation⁵,

$$h_r = \frac{\sigma \varepsilon (T_{\text{wall}}^4 - T_{\text{sat}}^4)}{T_{\text{wall}} - T_{\text{sat}}}$$

where σ is the Stefan-Boltzmann constant and ε is the surface emissivity. The total heat transfer coefficient is then calculated from³,

$$h = h_b + \frac{3}{4} h_r \quad \text{for } h_r < h_b$$

After all of the water in the tubes has boiled, the heat transfer becomes a function of free convection of a vapor similar to the free convection of the liquid state experienced prior to the onset of nucleate boiling.

CORRELATIONS IN REDUCED GRAVITY

As the thermal/fluid model was being developed, the question was raised as to the effects that microgravity may have on boiling heat transfer. Thus, a search of the relevant text was initiated. One of the first observations that were made after the research began was that the issue of boiling in a reduced gravity environment has been a topic of great debate among researchers. Testing has been conducted dating back to the 1950's when the only means of testing in a reduced gravitational field was in the form of drop towers⁷. These early drop towers were on the order of a few meters in height and provided barely a second of free fall simulating reduced gravity. However, later drop towers and drop shafts, which use abandoned mining shafts, increased dramatically in height. Many of these facilities now reach over a hundred meters or more in height, providing several seconds of quality reduced gravity on the order of $10^{-5}g$ with relatively little g-jitter (small oscillations in the mean g value). As an example, the JAMIC drop shaft in Hokkaido, Japan extends 790 meters into the ground and provides 10 seconds of free fall⁴. Other methods employed in simulating reduced gravity include parabolic flights aboard aircraft and sounding rockets which both provide even longer test periods on the order of 20 seconds for parabolic flights and up to 20 minutes for sounding rockets. While the sounding rockets provide good quality reduced gravity on the order of $10^{-4}g$, they are more expensive and the experimental apparatus must be fully automated. The parabolic flights provide relatively poor quality reduced gravity on the order of $10^{-2}g$ with an excessive amount of g-jitter; however, the experimental apparatus may be monitored and changed as needed during the experiment. In the last decade, experiments have been placed onboard space shuttle flights, which provide good levels of reduced gravity on the order of 10^{-4} to $10^{-5}g$ with jitter levels depending on crew movements and operation of onboard systems⁴.

Most of the experiments have been performed using a heated wire or horizontal flat plate immersed in a liquid, usually refrigerants such as R-113. However, some experiments have been

performed using water as the test liquid⁸. The results of the various experiments are often conflicting. One example of this is found when comparing the results produced by Lee et al.⁹ and Lee and Merte¹⁰ to the results produced by Oka et al.⁸. The results from the first two sources show an enhancement in the heat transfer coefficient in reduced gravity while the results of the later group show degradation in heat transfer. It is hard to compare the results of these two separate studies since the conditions under which they were obtained were so different. The experimental data produced by Lee and Merte¹⁰ were obtained for R-113 on 5 separate space shuttle missions as part of the NASA Get Away Special (GAS) program. These experiments were able to achieve multiple long duration steady state boiling test runs at various surface heat flux levels for saturated and sub-cooled boiling.

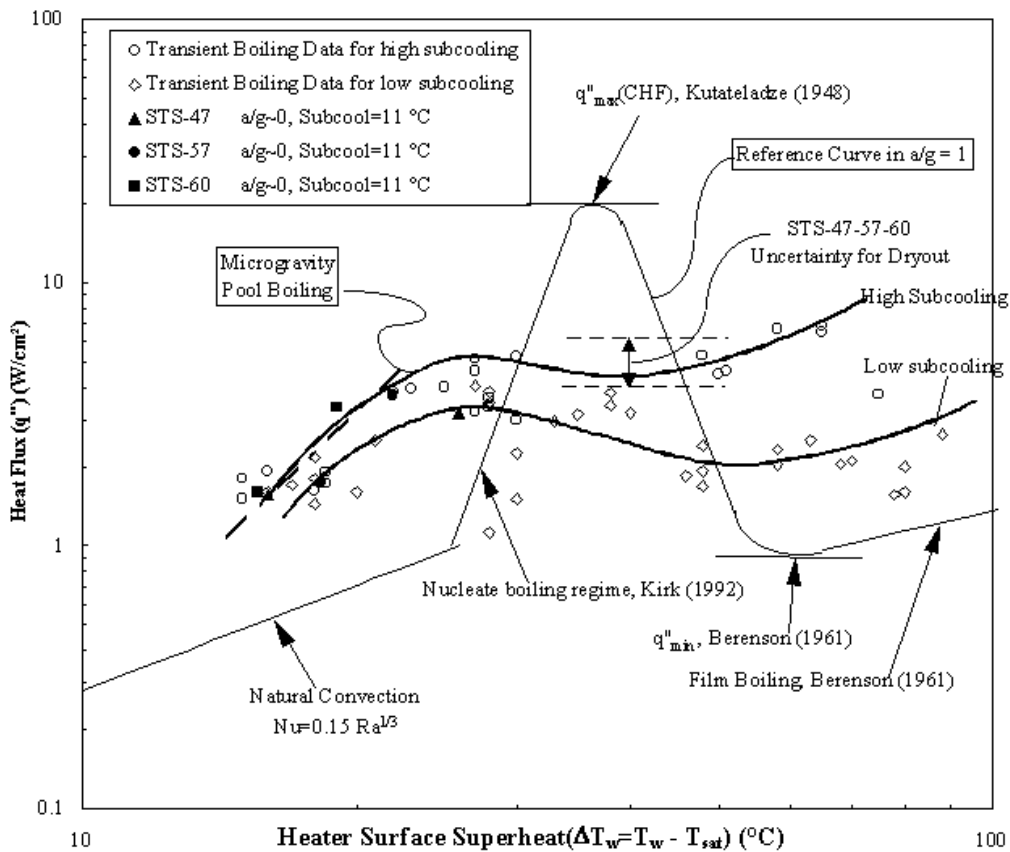


Figure 4: Reduced Gravity Pool Boiling Curve for R-113.⁹

Figure 4 shows the boiling curve produced by Lee et al.⁹ over the course of several shuttle missions. Lee and Merte¹⁰ have even produced a curve showing the derived heat transfer coefficient for reduced gravity as compared to terrestrial values (see figure 5). The experimental results produced by Oka et al.⁸ were obtained for both R-113 and water by using the drop shaft at the Japan Microgravity Center (JAMIC). The nature of these experiments did not allow for long duration test runs and thus steady state nucleation was not achievable. Both experiments were performed on a flat heating surface as opposed to a wire heater immersed in a fluid, which has shown yet another set of characteristics according to additional research teams⁴. One would

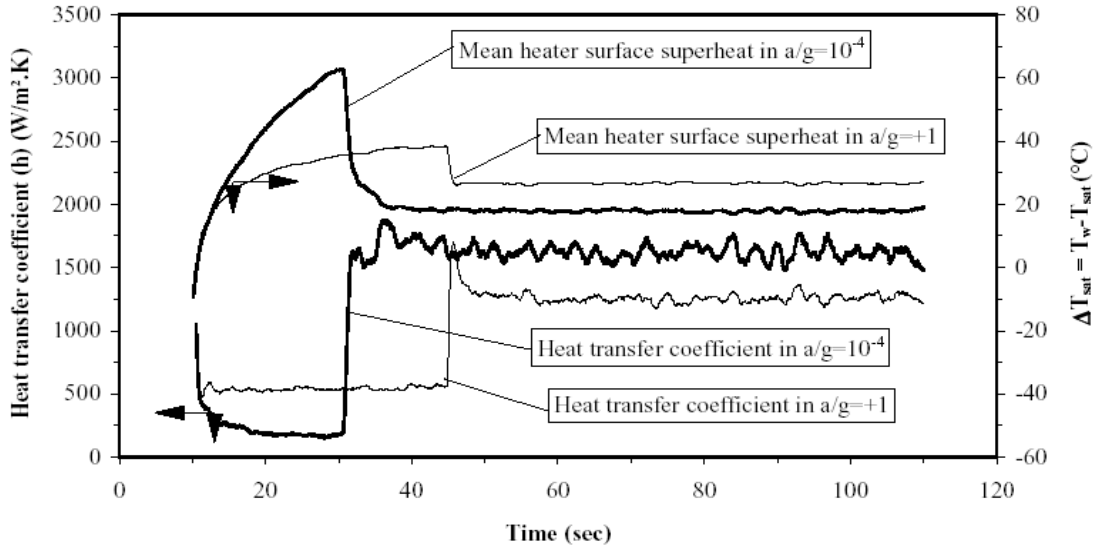


Figure 5: Mean Heater Surface Temperature and Derived Heat Transfer Coefficient

tend to be more confident in the results produced by Lee and Merte¹⁰ since their test data was produced in the same environment that the QMI will experience, i.e. low Earth orbit (LEO). The results of their experiment found that the onset of nucleate boiling occurs sooner in reduced gravity and that as much as a 32% enhancement in the heat transfer was observed and as much as 40% for high levels of sub-cooling, and the critical heat flux is substantially reduced⁹. Figure 6 shows a sequence of images of the experimental apparatus during nucleate boiling.

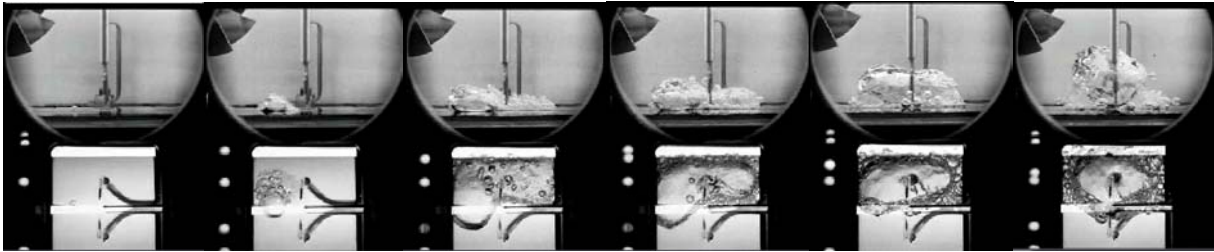


Figure 6: Sequence of Images of R-113 During Sub-cooled Boiling

Figure 7 is a sequence of images taken from the same experiment only with very low levels of surface heat flux. In this sequence of images the coalescence of the bubbles into a large single bubble is witnessed. The larger vapor bubble acts as reservoir for the smaller vapor bubbles, maintaining its size through the dual action of condensation and coalescence¹⁰.

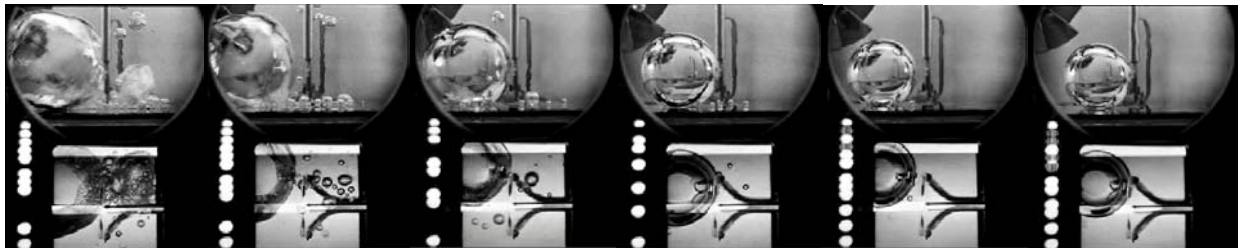


Figure 7: Sequence of Images of R-113 During Sub-cooled Boiling at Low Heat Flux Levels.

Unfortunately, most researchers are in mutual agreement that the heat transfer coefficients and the effect of reduced gravity vary for different fluids as well as for different surface geometry. Since the data produced by Lee and Merte¹⁰ is for R-113, it cannot be applied to the configuration of the QMI with any confidence. Since water has a surface tension roughly four times that of R-113 and a heat of vaporization on the order of 14 times greater, it stands to reason that the two liquids would behave very differently in reduced gravity where heat transfer is driven by surface tension effects on bubble formation and detachment behavior. As it stands in the current state of pool boiling reduced gravity research, the quantity of experimental data is insufficient to support the derivation of any form of heat transfer correlations. One researcher suggested that those types of correlations are still a decade away. Even then, any correlations that may be derived will continue to be updated as more and more research is conducted. This is still occurring with Earth based correlations today, some 60 years after the first correlations were developed.

While the desired analytical correlations are not available, what can be taken from this investigation is a general picture of the behavior of fluid heat transfer in reduced gravity. This information will allow ground-based analysis to be tailored as much as possible towards a more accurate solution. For example, in a reduced gravity environment, the convection phase prior to the onset of nucleate boiling will be replaced by pure conduction through the fluid. Furthermore, knowing that in reduced gravity the critical heat flux is lower and the transition to film boiling occurs more quickly enables us to determine in which direction the actual results will deviate from the analytical results. Knowing these characteristics can give us a better idea of what to expect during an actual “on-orbit” loss of cooling event.

MODELING RESULTS

While the reduced gravity research was very interesting, we are still left with the modeling issues of phase change heat transfer. Apart from actually placing the QMI test unit on the shuttle and performing a loss of cooling experiment, the ground-based correlations will have to suffice. As stated in the preceding paragraph, the single-phase convection correlations can be replaced with conduction through the fluid. This will at least simulate the effects of a microgravity environment prior to the onset of nucleate boiling. In SINDA/FLUINT, as the flow rate in tubes approaches zero, single-phase heat transfer conductances are applied assuming a laminar Nusselt number and a constant surface temperature defined by the equation²

$$Nu_D \equiv \frac{h \cdot D}{k} = 3.66 ; \text{ Laminar}$$

To simulate the conduction through the fluid in a microgravity environment the heat transfer is calculated from the radial conduction equation³.

$$hA = \frac{2\pi \cdot L \cdot k}{\ln(r_2/r_1)}$$

To simulate pool boiling, SINDA/FLUINT applies the above laminar Nusselt number equation to single-phase *vapor*, and to simulate condensation, the same equation is applied to single-phase *liquid*. This is a conservative method of calculating the heat transfer and greatly over-simplifies the boiling condition. SINDA/FLUINT does not perform a critical heat flux calculation; nor does it handle the case of sub-cooled boiling². These conservative methods used by the SINDA/FLUINT processor would produce results that are nearly the same as those produced by the original technique that was employed using the SINDA/G thermal model. In order to try and produce less conservative results that more realistically simulate the boiling heat transfer phenomenon, the internal correlations that are automatically called by the SINDA/FLUINT processor were replaced. The convection heat transfer ties described above were replaced by user heat transfer ties². By using these heat transfer ties in SINDA/FLUINT, the correlations discussed in the boiling section for Earth gravity could be incorporated. Prior to developing this model, a baseline case using the automated calculations of the SINDA/FLUINT processor was needed. This would allow the results from the user supplied correlation case to be compared to the results produced by the internal SINDA/FLUINT correlations. Attempts to obtain results from the baseline thermal/fluid model resulted in catastrophic failures of the SINDA/FLUINT processor. Whether using automated calculations or user inputs, the solution routine would not converge once phase change began in the fluid tanks. All attempts to resolve this issue had little or no effect. As the fluid in the tanks representing the chill block coil began to boil, increasingly smaller time-steps were taken by the FWDBCK solution routine. The model was allowed to run for several days to get past this transition at which point large fluctuations in the vapor temperature were observed. This pattern continued until boiling began to occur in the tanks around the furnace housing at which point the model began experiencing fluid property routine errors and the solution routine failed. Numerous modeling variations of Junction/Tank combinations were implemented in an attempt to resolve this issue. Attempts were also made using twinned paths and twinned tanks with ifaces. None of the methods employed had any positive effect (some actually made the problem worse). The control constants FRAVER, DTSIZE, RMFRAC, and RMRATE were adjusted in attempts to force the solution routine to smoothly pass through the phase change transition. This too had little or no effect. It was concluded that due to the overwhelming size and complexity of the thermal model the solution was unattainable with the current configuration. A model of this size requires a significant amount of processor time even without the added complication of a fluid submodel with phase change heat transfer. The SINDA/FLUINT manual warns users of the possible pitfalls of modeling phase change using tanks, stating, "*Small, two-phase or vapor (soft) tanks can significantly slow the solution.*"². Since one of the desired uses of this model was to track liquid volumes and associated expulsion rates during phase change, using junctions instead of tanks was not an option. Furthermore, junctions have no associated mass, and as a result no energy storage effects would be observed.

CONCLUSIONS

So what does all this mean for the situation of boiling in the cooling tubes on QMI? Essentially, there isn't enough data at this time to reliably incorporate any kind of analytical solution for reduced gravity boiling heat transfer. Furthermore, since the current configuration of the thermal/fluid model will not successfully run to completion in SINDA/FLUINT, the more

conservative approach will continue to be used were the assumption is that the water boils instantly with no phase change energy storage. Currently in development is a reduced order thermal model. The thermal nodalization has been reduced to fewer than 200 nodes. Once the reduction is complete and the model has been correlated to test data, the fluid model can then be integrated with the reduced model and another attempt will be made to achieve a solution with phase change heat transfer. Prior to this task, a stand alone fluid model representing both cooling loops will need to be run to ensure that the SINDA/FLUINT processor can effectively simulate simultaneous boiling in two separate locations in the water loop. Additional research is also needed in order to find more relevant ground based correlations for pool boiling in tubes. If the reduced version of the model is successful in simulating phase change, then the internal correlations will be replaced with the most appropriate ground correlations available. The results can then be compared to the baseline loss of cooling analysis and possibly presented in a future technical paper.

ACKNOWLEDGEMENTS

The author wishes to acknowledge the contributions of Shawn Breeding and Julia Khodabandeh, of the Marshall Space Flight Center, for their past modeling efforts from which the thermal/fluid model discussed in this paper was constructed.

REFERENCES

1. Breeding, S., et al., "Quench Module Insert Critical Design Review: Thermal Design Data Book", June 2000.
2. Cullimore, B.A., Ring, S.G. and Johnson, D.A., SINDA/FLUINT User's Manual, Version 4.3, June 2000.
3. Incropera, F.P. and DeWitt, D.P., Fundamentals of Heat and Mass Transfer, 3rd edition, John Wiley and Sons, 1990.
4. Di Marco, P. and Grassi, W., "Overview and Prospects of Boiling Heat Transfer Studies in Microgravity", *Proceedings of IN SPACE 97*, Tokyo (J), 18-19 November 1997.
5. Chapman, Alan J., Heat Transfer, 4th edition, Prentice Hall, 1984.
6. Collier, John G., Convective Boiling and Condensation, 2nd edition, McGraw-Hill, 1981.
7. Straub, J., Zell, M. and Vogel, B., "Pool Boiling in a Reduced Gravity Field", *Proceedings of the 9th International Heat Transfer Conference* (Jerusalem, Israel), Vol. 1, Hemisphere, New York, 1990, pp. 91-112.
8. Oka, T., Abe, Y., Mori, Y.H. and Nagashima, A., "Pool Boiling Heat Transfer in Microgravity", *JSME International Journal, Series B: Fluids and Thermal Engineering*, Vol. 39, No. 4, 1996, pp. 798-807.
9. Lee, H.S., Merte, H. and Chiamonte, F., "Pool Boiling Curve in Microgravity", *Journal of Thermophysics and Heat Transfer*, Vol. 11, No. 2, April-June 1997, pp. 216-222.
10. H.S. Lee and H. Merte, Jr., 1999, "Pool Boiling Mechanisms in Microgravity", *Proceedings of the Engineering Foundation Conference on Microgravity Fluid Physics and Heat Transfer*, Ed. V. K. Dhir, Oahu, Hawaii, September 19-24, 1999.

NOMENCLATURE, ACRONYMS, ABBREVIATIONS

Acronyms

CHF	Critical Heat Flux
ISS	International Space Station
LEO	Low Earth Orbit
MSRR-1	Materials Science Research Rack-1
MSL	Microgravity Science Laboratory
ONB	Onset of Nucleate Boiling
QMI	Quench Module Insert

Symbols

c_p	Constant Pressure Specific Heat
C_{sf}	Empirical Constant
D	Diameter
g	Acceleration of Gravity
h_{fg}	Heat of Vaporization
h	Heat Transfer Coefficient
k	Thermal Conductivity
L	Length
\ln	Natural Logarithm
n	Empirical Constant
Nu	Nusselt Number
Pr	Prandtl Number
q_s''	Surface Heat Flux
r	Radius
T_{wall}	Wall or Surface Temperature
T_{sat}	Saturation Temperature of the Liquid
ΔT	Temperature Difference
μ	Viscosity
ρ	Density
σ	Surface Tension, Stefan-Boltzmann Constant
ε	Surface Emissivity

Subscripts

b	boiling
l	liquid
r	radiation
v	vapor